Chapter 3

Fundamentals of Chemical Vapor Deposited Graphene and Emerging Applications

Golap Kalita and Masaki Tanemura

Additional information is available at the end of the chapter

http://dx.doi.org/10.5772/67514

Abstract

Graphene, the atomically thin sheet of sp^2 hybridized carbon atoms arranged in honeycomb structure, is becoming the forefront of material research. The chemical vapor deposition (CVD) process has been explored significantly to synthesis large size single crystals and uniform films of monolayer and bilayer graphene. In this prospect, the nucleation and growth mechanism of graphene on a catalytic substrate play the fundamental role on the control growth of layers and large domain. The transition metals and their alloys have been recognized as the active catalyst for growth of monolayer and bilayer graphene, where the surface composition of such catalysts also plays critical role on graphene growth. CVD-synthesized graphene has been integrated with bulk semiconductors such as Si and GaN for the fabrication of solar cells, photodetectors, and light-emitting diodes. Furthermore, CVD graphene has been integrated with hexagonal boron nitride (hBN) and transition metal dichalcogenides (TMDCs) for the fabrication of van der Waals heterostructure for nanoelectronic, optoelectronic, energy devices, and other emerging technologies. The fundamental of the graphene growth process by a CVD technique and various emerging applications in heterostructure devices is discussed in detail.

Keywords: graphene, CVD synthesis, atmospheric and low pressure, catalyst, graphene heterostructure

1. Introduction

Graphene was first introduced in 2004 by Prof. Andre Geim and Prof. Konstantin Novoselov by exfoliation of graphite using scotch-tape [1]. Prior to this ground breaking work, Peierls and Landau have predicted that the two-dimensional (2D) layered materials are thermodynamically unstable and difficult to find in nature [2–4]. The advent of atomically thin graphene revolutionized the 2D materials in physics, chemistry, and engineering fields, opening

enormous potential applications [5–10]. Considering the pioneering work on graphene, the 2010 Nobel Prize in Physics was awarded to Prof. Geim and Prof. Novoselov. Graphene can be considered as the main building block of various other forms of sp^2 hybridized carbon atoms (**Figure 1**). One of the most well-known allotrope is buckminsterfullerene also called as buckyball or fullerene (C_{60}), which was discovered in 1986 by R. F. Curl, H. W. Kroto and R. E. Smalley [11]. The soccer ball look-alike buckyball with a diameter only of 7.1 Å and consisting of 12 pentagons and 20 hexagons carbon rings. Its existence had been predicted earlier in 1970, by the Japanese theoretician Eiji Ozawa et al. [12]. Similarly, carbon nanotubes (CNTs), another form of carbon, have generated significant interest in the research fraternity due to their fascinating properties such as a one-dimensional (1D) structure [13]. In contrast to a buckyball, the CNTs can be considered as a rolled sheet of graphene forming 1D tubular structure. A rolled single sheet graphene will form single walled CNTs, while multiple rolled graphene sheet will create multi-walled CNTs. Graphene quantum dots (GQDs) and nanoribbons are also explored considering their unique characteristics [14, 15]. The discussed various forms of crystalline carbon in different dimensions (i.e., zero, one, two, and three dimensions) exhibit contrasting physical and chemical properties and are prominent materials for wide

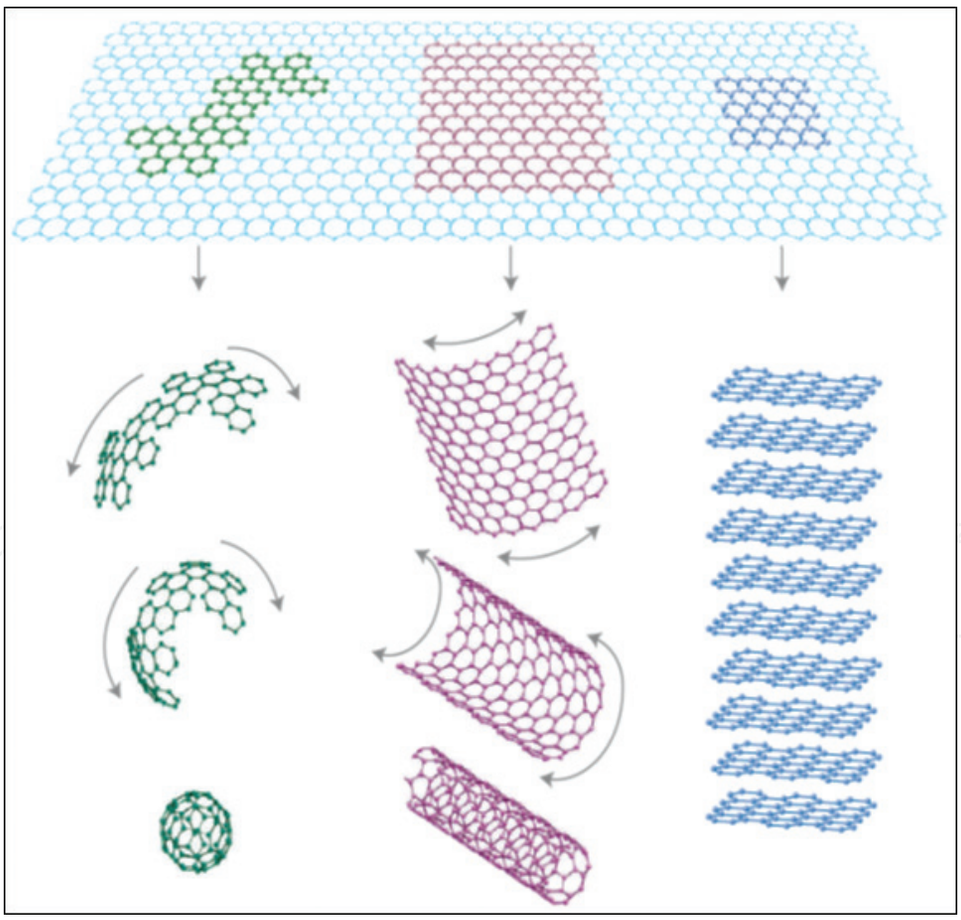

Figure 1. 2D graphene sheet is the building block of other forms of sp^2 hybridized carbon in all other dimensions. The graphene sheet can be wrapped to form fullerene (zero dimension), rolled into nanotubes (one dimension), or stacked into graphite (three dimension). [Reprinted with permission from Ref. [9]].

http://dx.doi.org/10.5772/67514

range of applications. Various physical phenomena and structure-related properties have been explored or discovered, while graphene can be ideal form of the materials to understand the various other forms. In the chapter, we focused on graphene growth process on catalyst substrates by the low and atmospheric pressure CVD process. Subsequently, we emphasize on different possible catalysts for graphene growth and their surface structures for selective growth of monolayer, bilayer, and large single crystal domains. Recent development and emerging applications of CVD graphene for the fabrication of heterostructures with bulk semiconductor and van der Waals heterostructures with other two-dimensional (2D) materials were introduced and explained.

2. Crystal structure and basic properties of graphene

The unit cell of graphene contains two carbon atoms and the graphene lattice can be considered to be made of by two sublattices, A and B (**Figure 2(a)**). The A and B sublattices are triangular Bravais lattices; therefore, the graphene honeycomb lattice can be viewed as a triangular Bravais lattice also called as hexagonal lattice with a two-atom basis (A and B). **Figure 2(a)** shows the honeycomb lattice of graphene. The vectors δ_1, δ_2, and δ_3 connect nearest neighboring carbon atoms, separated by a distance of a = 0.142 nm. The vectors a_1 and a_2 are basis vectors of the triangular Bravais lattice. The reciprocal lattice of the triangular lattice with primitive lattice vectors a^*_1 and a^*_2 is presented in **Figure 2(b)**. In the center, the shaded region represents the first Brillouin zone, with its center Γ, and the two inequivalent corners K (black squares) and K′ (white squares). The π-bands electronic dispersion relations for the 2D honeycomb crystal lattice of graphene under the tight binding (TB) approximation is shown in **Figure 2(c)**. Plots are shown for the electron energy dispersion for π and π*-bands in the first and extended Brillouin zones as contour plots at equidistant energies and as pseudo-3D representations for the 2D structures. Electronic band structure can be simply presented by a Dirac cone, where the valance and conduction band touch at Dirac point [16]. The cone-shape energy band structures present linear electronic dispersion and density of states (DOS) of graphene, which significantly differ from conventional metals and semiconductors.

The quantum confinement of the electrons in absence of a third dimension provides graphene various exciting properties. Electrons in graphene behave as massless relativistic fermions at low temperatures, which is an unusual behavior for condensed-matter system [16]. Graphene shows an unusual (relativistic) quantum Hall effect with an applied perpendicular magnetic field at a temperature as high as room temperature [6]. The massless Dirac fermion (i.e., charge carrier) of graphene moves at ballistic speed in submicron length, close to relativistic speeds. It has been estimated that the intrinsic carrier mobility of graphene is as high as 200,000 $cm^2\ V^{-1}s^{-1}$ [18]. The 2D graphene sheet is also known to be an excellent current conductor; the sustainability of current density is six orders higher than of normal Cu [9]. Graphene also shows exceptional mechanical strength, with breaking strength of ~40 N/m and the Young's modulus of ~1.0 TPa [8]. The thermal conductivity of a suspended graphene sheet at room temperature has been measured as in the range of 4.84×10^3–5.3×10^3 W/mK [19]. The absorption coefficient of graphene has been determined from the fine structure constant ($\alpha = e^2/\hbar c$), which signifies that the absorbance and

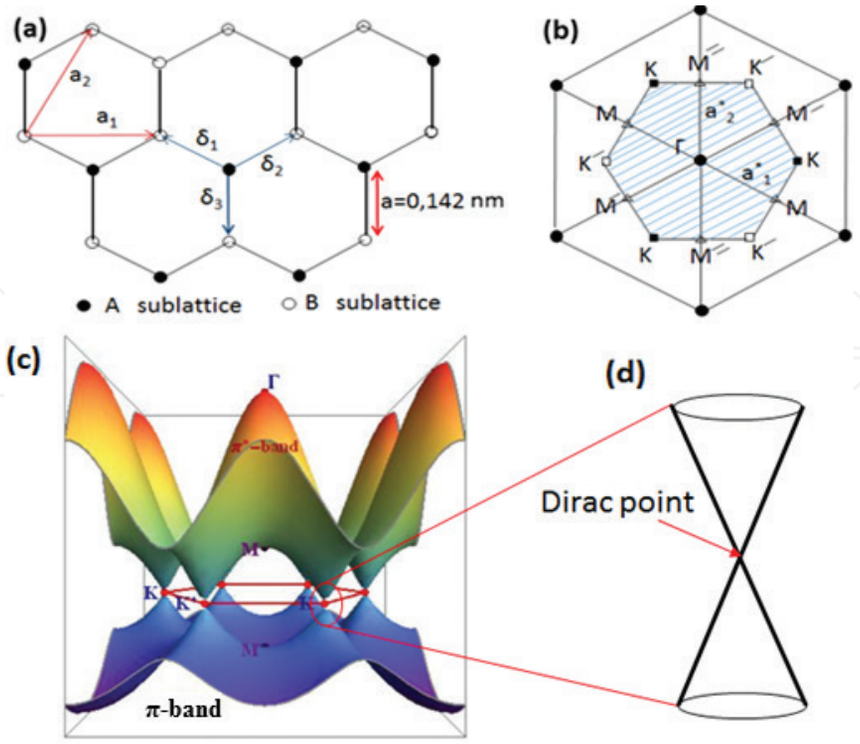

Figure 2. (a) Two graphene sub-lattices (A and B) and unit cell. (b) Reciprocal lattice of the graphene lattice, presenting the Brillouin zone, and (c) π-bands electronic dispersion relations for a 2D honeycomb crystal lattice of graphene under the tight binding (TB) approximation (http://demonstrations.wolfram.com/GrapheneBrillouinZoneAndElectronicEnergyDispersion). (d) Electronic band structure and presentation of Dirac point of 2D graphene crystal.

transparency of graphene is independent of wavelength. A monolayer graphene absorb 2.3 ± 0.1%; of the incident light with a negligible reflectance of <0.1% [7]. Graphene, with only one atomic layer, has a high surface area-to-volume ratio without affecting much of the mechanical properties. In the chemistry point of view, graphene sheets can be functionalized with other elements to achieve heterogeneous chemical and electronic structures. The basic properties of graphene-based material are summarized in **Table 1**.

Properties	Graphene	References
Electrical	• Band structure for Graphite • Carrier mobility~200,000 $cm^2\ V^{-1}s^{-1}$ • Unusual (relativistic) quantum Hall effect • Excellent conductor (Can sustain 6 orders higher current than Cu)	Wallace [17] Morozov et al. [18] Zhang et al. [6] Geim and Novoselov [9]
Optical	• Graphene absorb 2.3 ± 0.1% of light (From fine structure constant), independent of wavelength	Nair et al. [7]
Thermal	Thermal conductivity~4.84 × 10^3 to 5.3 × 10^3 W/mK	Balandin et al. [19]
Mechanical	Breaking strength of ~40 N/m and Young's modulus of ~1.0 TPa	Lee et al. [8]
Chemical	Functionalization with various functional groups	Loh et al. [20]

Table 1. Properties of graphene 2D crystals.

http://dx.doi.org/10.5772/67514

3. Synthesis of graphene-based materials

The first demonstrated process to derive graphene was exfoliation of graphite by using a simple scotch tape technique [21]. The repeated exfoliation on a substrate surface enabled to derive a very thin sheet consisting of few-layers graphene. The unique physical properties of the exfoliated 2D graphene sheet led to several outstanding innovations in graphene deriving and synthesis process. Mechanical exfoliated graphene has been widely studied to investigate physical properties of graphene and electronic device fabrication [8–12, 21]. The scotch tape technique produces only a few micron sheet, which has only limited application prospective. Again, the technique is time consuming and basically depends on trial and error approach with difficulties to locate with repeatability. The other well-known approach explored in the very beginning of the graphene research is epitaxial growth on silicon carbide (SiC). Graphene on SiC has been synthesized by high temperature annealing process (>1300°C) in high vacuum chamber [22, 23]. In the annealing process, top layer of SiC undergoes thermal decomposition, where Si atoms desorb and carbon atoms remain on the surface rearranging and bonding to form sp^2 hybridized graphene structure. The main drawback of graphene growth on SiC is small domain structures with the presence of steps and terrace edges. Again, the high cost of SiC substrate and high processing temperature in vacuum chamber make less industrial attractive. The other alternative approach is reducing of chemically exfoliated graphene oxide (GO) to derive large quantity of graphene flakes [20, 24]. GO has been synthesized at around room temperature by a modified Hummer method that involves rigorous oxidation of pure graphitic materials [25, 26]. The oxygen-related functional groups enhance the interlayer distance of graphene sheets of graphite, which make it possible to exfoliate readily with reduce van der Waals interaction between the layers. GO is an insulating graphene sheet containing epoxy and hydroxyl oxygen functional groups on the basal plane and at the edges [27–29]. GO-based materials are electronically hybrid material that features both π state of sp^2 carbon and the σ state of sp^3 bonded carbon with oxygen. Controlling the sp^2 and sp^3 hybridized carbon atoms ratio with oxidation and reduction process the desirable optical and electronic properties can be achieved [20]. However, significant structural defects are induced in the graphene lattice with reduction of GO, which considerably effect the mechanical and electrical properties. Although the chemical exfoliation and reduction process can be carried out at room temperature to synthesize a large quantity of graphene, it does not satisfy the norms for electronic grade materials. Nevertheless, there are various possibilities for composite and electrode materials for energy conversion and storage devices.

In the above-discussed point of views, the CVD process is one of the most prominent approaches for the synthesis of high quality graphene with a controlled number of layers in large area. In the CVD approach, hydrocarbons are decomposed and catalyzed to form sp^2 hybridized carbon for lateral growth on a substrate. Graphene can be synthesized with desired structures depending on the CVD process, catalyst substrates, nature of precursors, base pressure, and gas composition. Recent significant development of high-quality and single crystal graphene synthesis by the CVD technique on metal substrates opens up new possibilities for applications [32–37]. In the following, we discuss in detail about the CVD synthesis process and growth mechanism of graphene on various catalyst substrates.

4. Development of chemical vapor deposition process

Growth of the graphitic layer on a transition metal substrate owing to atomic carbon segregation has been well known for many years [30]. Synthesis of planar nanographene (PFLGs) was demonstrated by Somani et al. by a simple CVD technique [31]. The graphitic structure included about ~35 layers of graphene, due to high segregation of carbon atoms on the Ni foil. The process was further developed to achieve control growth of monolayer, bilayer, and few layer graphene on the Ni-deposited SiO_2/Si and Ni foil [32, 33]. The main challenge of CVD graphene structure is to remove and transfer on an insulating substrate for physical properties characterization. In the later stage, transfer process of CVD graphene onto an arbitrary substrate without disturbing the intrinsic properties has been developed [34]. Transferring of a CVD graphene can be achieved by wet or dry etching of the catalytic layer and placing on a desirable substrate surface. The CVD process has been significantly explored to grow large size single crystals and high quality wafer-scale monolayer and bilayer graphene. In this prospect, the nucleation and growth mechanism of graphene on a catalytic substrate play the fundamental role in the formation of large domains and number of layers. The transition metals, alloys, and liquid metals have been recognized as the catalyst for growth of monolayer and bilayer graphene, where the surface composition of solid catalyst substrates also plays critical role on graphene growth. The thermodynamic and kinetic parameters are also crucial in graphene growth process, where pressure and temperature are both key factors [32–39]. The graphene growth mechanisms are discussed for the atmospheric and low pressure CVD technique in the following section.

5. Atmospheric and low pressure CVD technique

The atmospheric pressure chemical vapor deposition (APCVD) system consists of horizontal quartz tube connected to gas inlet and outlet [40]. **Figure 3(a)** and **(b)** presents schematic of two different possible APCVD and low pressure CVD (LPCVD) system depending on the precursor materials. Gaseous precursors can be supplied from external sources, while solid and liquid precursors can be directly inserted in the CVD chamber for graphene growth. The growth chamber pressure in graphene growth has been significantly explored to control the nucleation density and number of layers [41–45]. It has been observed that the activation energy of nucleation dramatically affects by the pressure i.e., different for the APCVD and LPCVD techniques. The effect of chamber pressure on graphene nucleation has been explored on Cu catalyst substrate, considering the self-limiting behavior for monolayer graphene growth on Cu [43–45]. It has been observed that the graphene nucleation density affected by several fundamental processes occurred on the Cu surface. These are: (i) precursor adsorption, (ii) formation of active carbon species (dehydrogenation), (iii) diffusion of active carbon on the surface, and (iv) critical size nuclei formation that competes with (v) desorption. Now, most of these processes are affected by the background pressure of CVD and responsible for the difference between the low and atmospheric pressure growth of graphene [45]. The overall pressure significantly affects desorption of various species from the catalyst surface. It has been explained that due to the collisions with the buffer gas in the diffusion layer close to the surface, the desorbed species have a higher returning

rate to the surface at higher pressures. The effect is inversely proportional to the background pressure, making the evaporation rates at atmospheric pressure more than 3 orders of the magnitude lower than at reduced pressures. In LPCVD process, diffusion of the gas decreases proportionally to the reciprocal of the pressure. The pressure for LPCVD system is typically ~10–1000 Pa, while the standard atmospheric pressure is 101,325 Pa. If the pressure in the CVD process is reduced from atmospheric pressure to about 100 Pa the diffusion will decrease by almost 1000 times [46]. Hence, the velocity of mass transport will reduce to the substrate surface inside growth chamber, allowing uniform and homogenous growth of graphene. Thus, graphene growth is less dependent on mass transport velocity in the LPCVD process [45, 47].

It has been reported that the carbon atoms adsorption energies on a Cu surface vary within 4.1–7.5 eV range, where graphene nucleation on the catalyst substrate significantly depends on desorption/etching of small active carbon species. It has been also reported that the Cu evaporation rate in vacuum is significantly high, which is around 4 μm/hour at 1000°C [48]. The high evaporation rate of Cu in a LPCVD process promotes desorption of carbon species adsorbed on top of the catalyst, leading to a lower nucleation density. The reported activation energy of nucleation, E_{nuc} ~ 3–4 eV at low pressures and temperature >950°C [45, 47]. On the other hand, sublimation of Cu in the APCVD process is significantly less, which lead increased activation energy for Cu atoms desorption as well as desorption energy of carbon atoms from the catalyst surface (E_{nuc} ~ 9 eV) [45]. Thus, graphene nucleation and growth significantly differ depending on the pressure of the CVD chamber affecting absorption and desorption of carbon atoms (**Figure 4**). Along with Cu, various other catalyst substrates have been explored for uniform monolayer or bilayer graphene growth in the CVD process as discussed below.

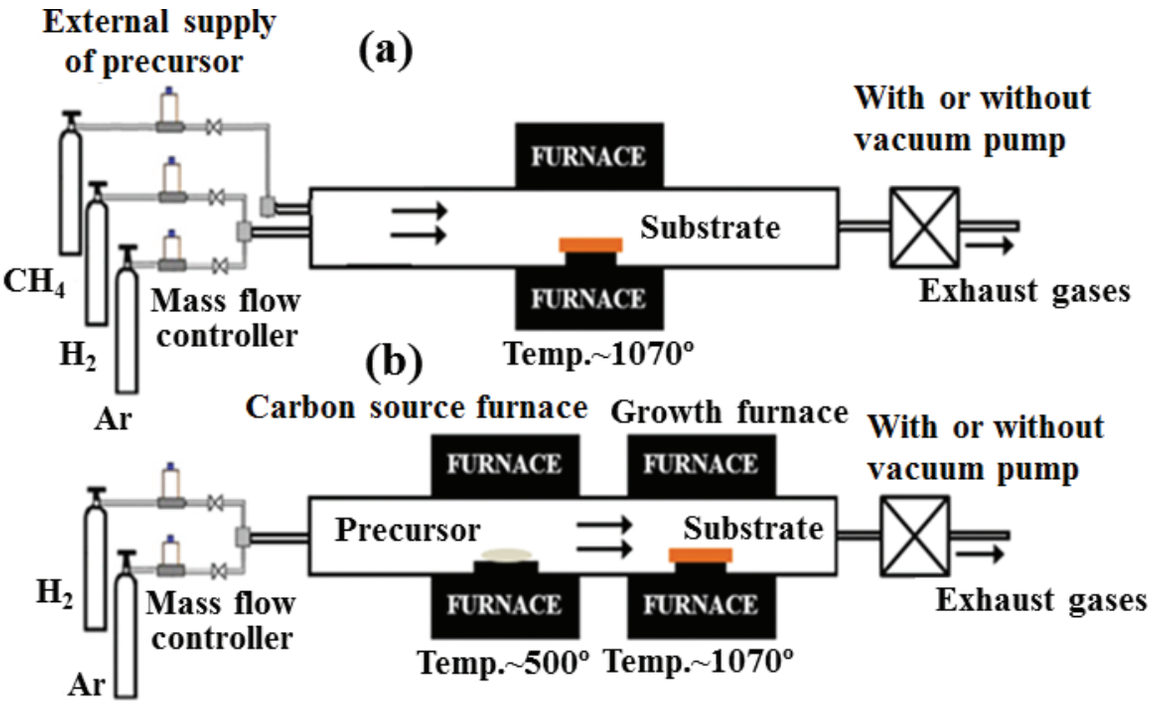

Figure 3. Two different possible CVD systems depending on the precursor materials. (a) External supply of gasses precursor and (b) Directly inserted solid and liquid precursors in APCVD and LPCVD modes.

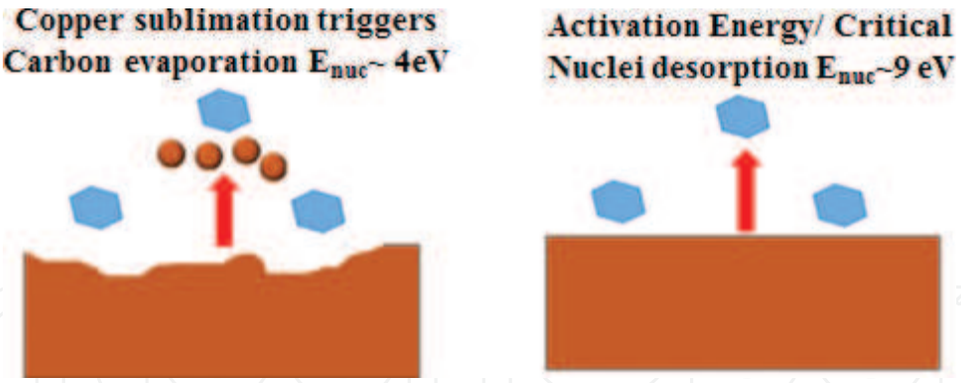

Figure 4. Activation energy differ for low and atmospheric pressure CVD. At low pressure, evaporation of Cu is significant which limits nucleation of graphene (E_{nuc} ~ 4 eV). Cu evaporation is less at atmospheric pressure CVD, where nucleation activation energy is higher (E_{nuc} ~ 9 eV). [Reprinted with permission from Ref. [45].

6. Catalysts for CVD process

6.1. Single transition metal catalyst

The CVD growth of graphene has been mostly investigated on transition metal catalysts (Ni, Cu, Co, Pt, Ag, Ru, Ir, Pd, etc.) [31–39, 49–53]. Growth of pyrolytic carbon films or layers of graphite have been first observed on Ni catalyst with introduction of hydrocarbon or evaporated carbon materials [30, 54]. Almost at the same time, the formation of graphitic layers on single crystal Pt and Ru was observed in catalysis experiments. The formation of graphitic layers can be explained with diffusion and segregation of carbon impurities on the metal surface during the annealing and cooling process. At an elevated temperature, hydrocarbons were thermally decomposed and surface absorption/desorption or segregation of carbon occur depending on carbon-metal solubility for graphene growth. The above-discussed (Section 5) absorption/desorption of carbon atoms for particular catalyst substrate can significantly differ, depending on carbon solubility on metal surface. Again, the metal catalyst can be polycrystalline or single crystalline in nature. The grain boundaries, crystallographic orientation of grain can significantly influence the absorption/desorption or segregation of carbon atoms, which leads diverse morphologies of graphene on different metal catalysts. In the following, we discussed two simple model of graphene growth process on highly carbon soluble Ni and low carbon soluble Cu catalyst. The stability and the reactivity of Ni at high temperatures, as well as its high carbon solubility (0.6 weight % at 1326°C), have been explored for graphene growth in the initial stage of CVD research [55]. The lattice constant of Ni is 3.52 Å and its first-neighbor distance in the bulk is 2.49 Å, which is almost identical to the lattice constant of graphene 2.46 Å [55, 56]. **Figure 5(a)** shows the growth model of graphene on the Ni catalyst. Bulk diffusion of carbon atoms can be dominant depending on the CVD growth conditions for high carbon soluble transition metal catalysts (**Figure 5(a)**). The nonequilibrium process leads to the carbon precipitation on the surface and the formation of graphene during the cooling down process [56–59]. It is difficult to obtain uniform graphene films with minimal microstructural defects on polycrystalline Ni, owing to multiple nucleation and unpredictable

http://dx.doi.org/10.5772/67514

quantity of segregated carbon. Contrary to the Ni catalyst substrate, Cu has a filled 3D shell that results in a low carbon solubility (0.008 weight % at 1084°C) and reduces the tendency for adsorbing hydrocarbons onto the Cu surface [60–62]. This favors an extensive surface migration of carbon adatoms on the Cu surface and a minimum diffusion into the bulk of Cu. The low affinity of carbon for Cu is also shown in the absence of carbide formation. The lattice constant of Cu is 3.61 Å and its first-neighbor distance in the bulk is 2.56 Å, which is slightly different than the lattice constant of graphene which is 2.46 Å. The lattice mismatch is around 3.7%, larger than of between Ni and graphene (1.2%), which indicates favorable growth on the Cu surfaces but with easier transfer due to the weaker interactions between graphene and Cu substrate. The carbon source precursor molecules are decomposed before being adsorbed by the Cu catalyst where the dehydrogenation of the molecules takes place, followed by the surface migration and the growth (**Figure 5(b)**) [62–64]. Growth conditions and substrate grain orientations of Cu also influence the growth of the graphene crystals. Considering the effect of catalyst substrate polycrystalline nature, epitaxial growth of graphene on single crystal Ni (111) and Cu (111) has been also explored [65–67]. Graphene can be grown with a preferred orientation on Cu(111), and even seamless sticking of graphene domains on Cu(111) substrates has been obtained. Thus, unidirectional alignment of nucleated graphene crystals on a single-crystal metal

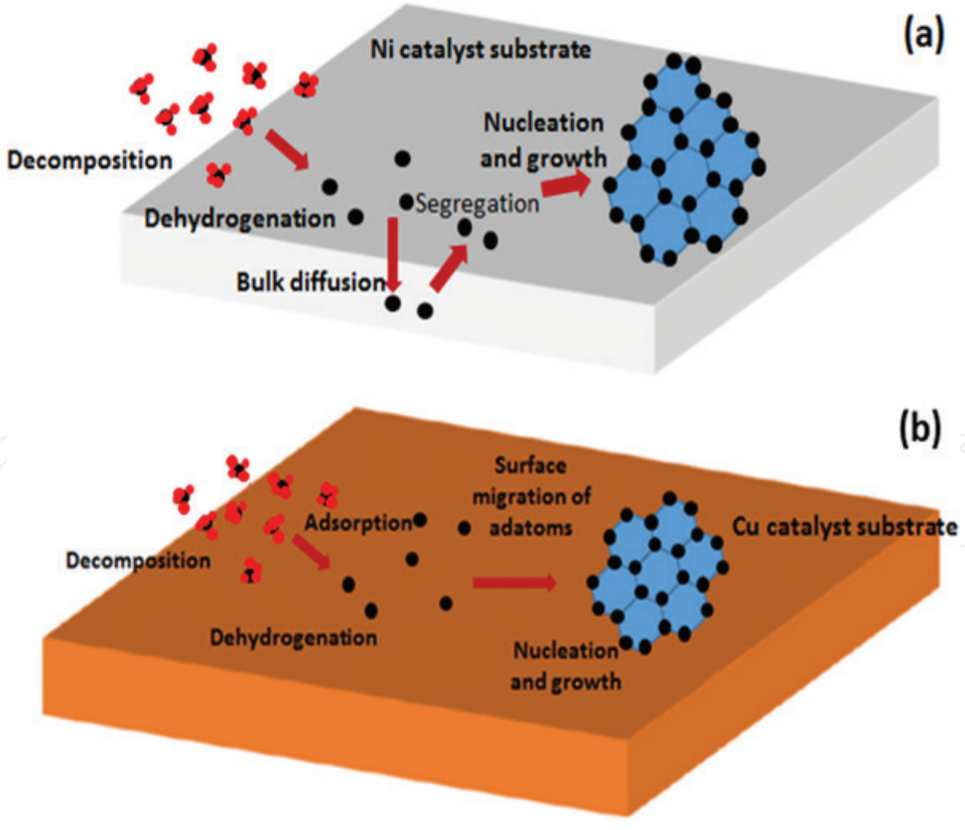

Figure 5. (a) Graphene growth process on highly carbon soluble metal substrate (e.g., Ni). Decomposition, dehydrogenation, bulk diffusion, and segregation process determined the graphene nucleation and growth. (b) Graphene growth process on a low carbon soluble metal substrate (e.g., Cu). Decomposition, dehydrogenation, and surface adsorption/desorption process determined the graphene nucleation and growth.

substrate can be the perfect solution to grow uniform graphene films. However, Synthesis of graphene on a single-crystal metal substrate is not suitable for large-scale production owing to the high cost and the difficulty of preparing single-crystal metal. Significant effort has been also made to synthesis large single crystal graphene on the metal catalyst to overcome the limitation of smaller graphene domain and polycrystalline nature [68–74]. In this prospect, modification of the Cu substrate surface by oxidation has enabled to reduce nucleation density, which allows large-area lateral growth of the same crystal (**Figure 6**) [72]. The processing of the Cu substrate surface is critical as well as the growth of kinetic parameters determine the size and shape of the single crystals. The main challenge toward this research prospect is to produce continuous large-area film with the same large size single domains in a less growth duration.

6.2. Binary transition metal catalyst

One of the important aspects, we learn from the above discussion, is that the traditional polycrystalline or single-crystalline metal catalysts have enabled the growth of uniform graphene film by complex pretreatments or precise parameter controlling. Rational designing of a binary catalyst can be significant to control nucleation density, number of layers, solubility of carbon and dopant, which will provide significant control in the CVD growth

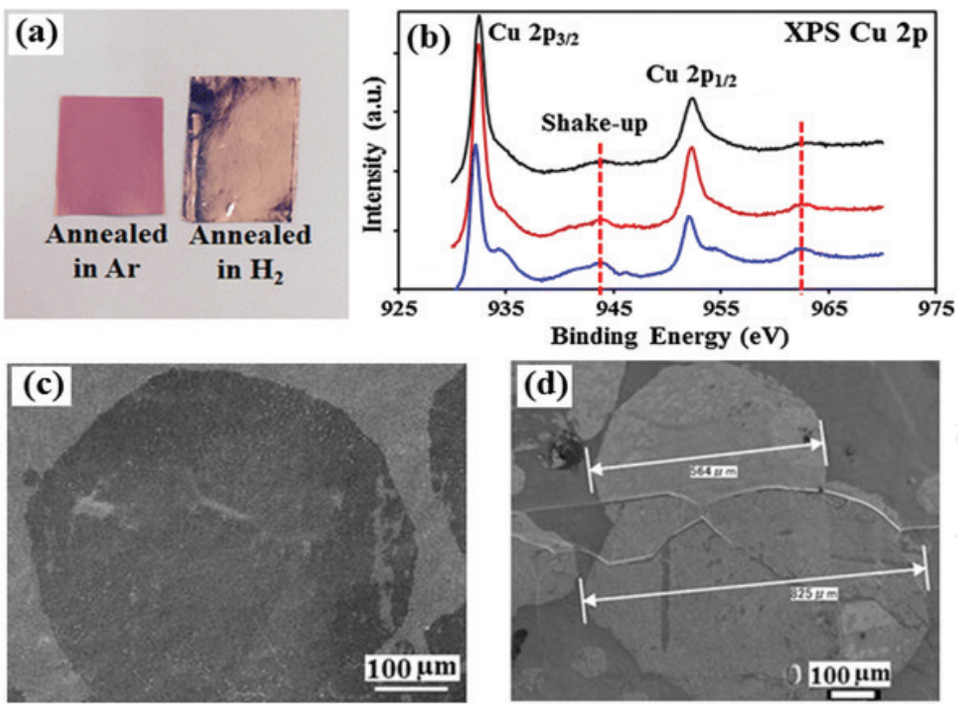

Figure 6. Oxidizing treatment of Cu for large domain growth. (a) Photographs of Cu foils after the annealing treatment in Ar and H_2 atmospheres. (b) XPS spectra of the Cu surface at different stages of the annealing. (c) SEM images of a large graphene domain (~510 µm). (d) Formation of millimeter scale structures with merging of two graphene domains (560 and 825 µm). [Reprinted with permission from Ref. [72].

http://dx.doi.org/10.5772/67514

process. Bilayer graphene with AA, AB stacking and rotation stacking fault is interesting prospect to observe novel physical properties (**Figure 7(a)**) [75–77]. It has been demonstrated that applying a vertical electric field in bilayer graphene-based field effect transistor (FET), a bandgap of the order of 0.2–0.3 eV can be observed [78]. Significant research effort has been given for control growth of bilayer graphene using a binary alloy catalyst to adjust the solubility of the carbon atoms. The solubility of carbon species at high temperature in Cu and Ni is significantly different, which leads to distinct growth behavior as discussed in Section 6.1. Growth of bilayer graphene can be achieved on Cu-Ni alloys with more than 90% coverage adjusting the Ni concentration in the alloy [79]. Synthesis of a highly uniform bilayer graphene film by the CVD process has been also achieved on an epitaxial Cu-Ni (111) binary alloy catalysts [80]. In the case of the epitaxial Cu-Ni alloy also the relative concentration of Ni and Cu as well as the other thermodynamic and kinetic parameters such as temperature, cooling profile, and gas composition strongly influence the uniformity of bilayer graphene growth. The other metal alloy such as Ni-Mo, Au-Ni, Co-Cu, etc. also can be significant to achieve control growth of graphene in a CVD process [81–84]. The present challenges toward this direction are selection of proper metal for alloy, composition, and alloy preparation techniques for further development. Significant effort has been also made to design alloy-based catalyst to achieve faster growth of larger graphene domains [85]. The binary alloy catalyst also facilitates to control the solubility of carbon and dopant atoms to achieve substitutional doping. Remi et al. have demonstrated that

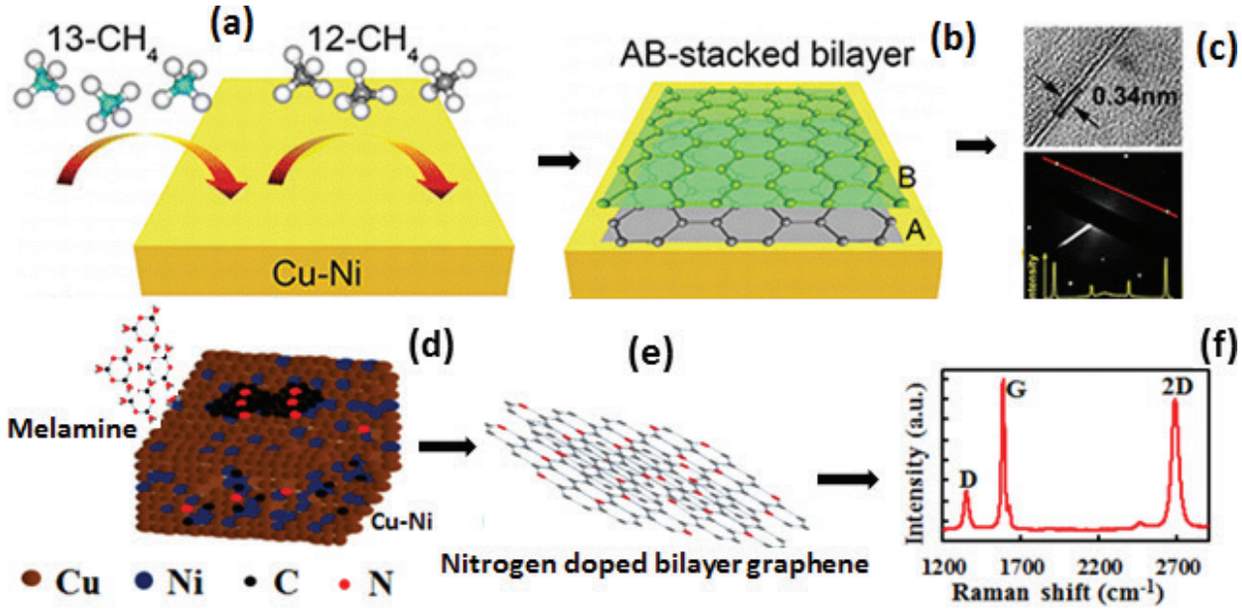

Figure 7. Graphene growth on the Cu-Ni binary alloy catalyst substrate by a CVD technique. (a) and (b) Schematics of the CVD growth process of AB stacked bilayer graphene on the Cu-Ni alloy. (c) Transmission electron microscopy (TEM) and diffraction analysis of the graphene. [Reprinted with permission from Ref. [76]]. (d) and (e) Schematic of nitrogen-doped bilayer graphene growth on the Cu-Ni binary alloy using a melamine solid precursor and (f) Raman spectra of the bilayer domain. [Reprinted with permission from Ref. [86]].

large nitrogen-doped bilayer graphene domains can be synthesized on the Cu-Ni binary alloy as shown in **Figure 7(b)** [86].

6.3. Liquid metal catalyst

Unidirectional nucleation and growth can be achieved on a liquid metal in the absence of a crystalline lattice and amorphous atomic structure, which is truly homogeneous [87, 88]. The quasi-atomically smooth surface of the liquid to avoid defects or grain boundaries such as those found in solid metals can be perfect choice for single layer graphene growth in the CVD process. The perfectly smooth liquid surface supports uniform nucleation and growth of graphene. The growth of graphene governed by a self-limited surface catalytic process and is robust to variations in CVD growth conditions [89, 90]. Homogenous monolayer graphene growth on liquid metals has been achieved using the CVD process. The p-block element, such as liquid Ga, has been also demonstrated as an attractive option for large high-quality graphene growth and expanding the catalyst family for graphene growth beyond d-block transition metals. Growth of monolayer graphene on liquid indium (In) and gallium (Ga) has been demonstrated, without the formation of sublayers as shown in **Figure 8** [90]. Thus, the development of various catalysts for the CVD process and achieving growth of graphene with desired numbers of layer, crystalline structure, and morphology with the highest quality will enable commercial applications. The comparison of various catalyst types for the graphene growth process is summarized in **Table 2**.

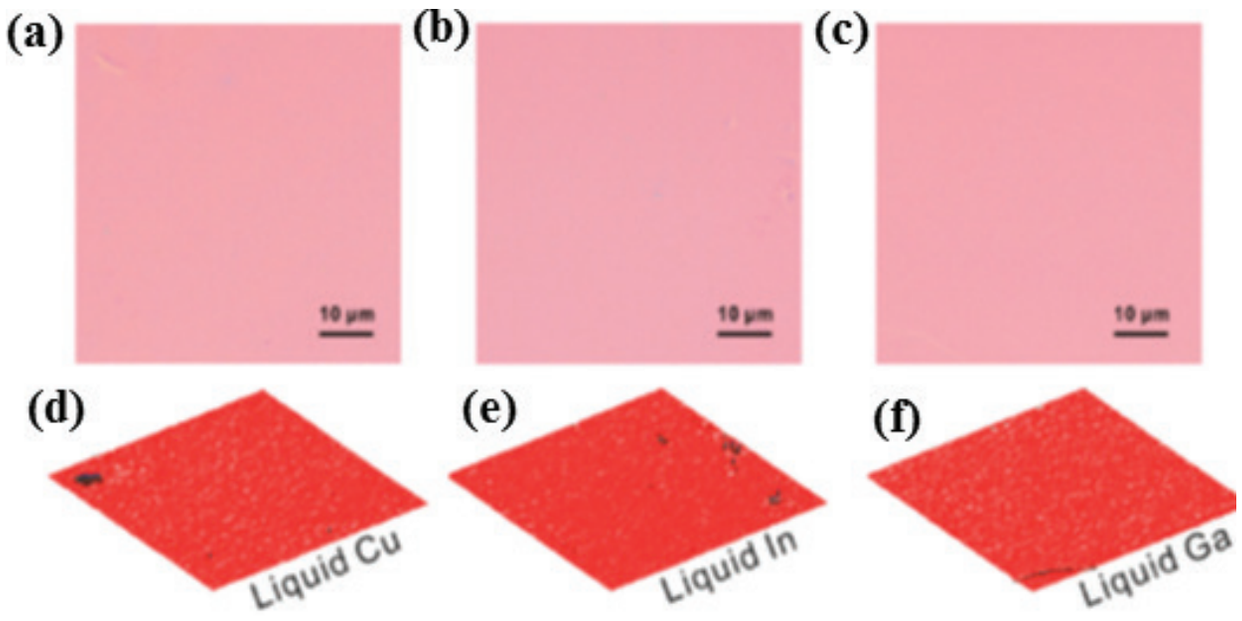

Figure 8. Typical growth results on liquid metal substrates. (a–c) Optical microscope images of graphene grown on liquid Cu, In and Ga respectively, which demonstrates the excellent uniformity of the single-layer graphene. (d-f) Layer distribution determined by RGB color analysis of the corresponding optical microscope images [Reprinted with permission from Chem. Mater. 2014; 26(12): 3637-3643].

Type of catalysts	Merits	Demerits
Polycrystalline metal	1. Low cost	1. Nonuniform growth
	2. Easy processability	2. Multilayer growth
	3. Simple CVD approach	3. Defect in grain boundaries
Single crystal metal	1. Unidirectional nucleation	1. Difficult to produce large area graphene
	2. Uniform monolayer	2. High processing cost for single crystal metal preparation
Binary alloy	1. Control layer growth	3. Alloy preparation technique
	2. Controllable doping of graphene	4. High processing cost
Liquid metal	1. Uniform single layer graphene	1. Handling and processability
		2. Transfer process (for example, transferring from liquid Ga surface)

Table 2. A comparison of catalyst types for various graphene growth process.

7. Heterostructure of CVD graphene with other semiconductors

The heterostructure of CVD graphene with other bulk and two-dimensional (2D) semiconductors has been developing extremely fast. Novel heterostructure devices are in main focus for solar cell, light-emitting diodes, photodetectors, gas sensors, tunneling transistors, resonant tunneling diodes, etc. [91]. This has enabled to utilize and integrate the properties of different materials to fabricate new highly efficient device architecture. Graphene with excellent electrical conductivity, tunable work function, doping to obtain p-type and n-type and high optical transparency has significant potential to combine with other semiconductor to fabricate novel devices. In the earlier stage, graphene considered to suitable transparent conductor for touch panel devices and as an alternative to metal oxide-based transparent conductors. Recently, applications of graphene have spread into many other areas, such as nanomechanical systems, nonvolatile memory, optoelectronics, interconnections, thermal management, and bioelectronics. Among these applications, graphene-based solar cells, photodetectors, light-emitting diodes are the most interesting because of their remarkable performances as transparent electrodes and active layers for photoelectric devices, which make them promising solutions for fast-response and energy-efficient applications. In the following sections, we discuss elaborately various CVD graphene-based heterostructures.

7.1. Graphene-Si heterostructure

Heterojunction of CVD graphene and Si has been extensively studied for solar cells and photodetector applications [92]. The transparency of CVD graphene in a wide wavelength range makes it possible to fabricate a broad wavelength range photodetector and utilize much higher solar light to achieve high conversion efficiency. Again, the density of state (DOS) for graphene significantly differs than that of conventional metals. It can be observed

that conventional metal has a finite DOS near Fermi energy, whereas graphene has a zero DOS at the Fermi energy (as discussed in Section 2). The unusual optoelectronic properties of graphene open new opportunities in device engineering than that of conventional metal-semiconductor-based devices. The CVD graphene on n-Si can create a Schottky junction with a large build-in potential due to its suitable work function as well as prospect to tune the barrier height. CVD synthesized a large-area monolayer or few-layer graphene has been transferred on the n-Si or p-Si substrate to create a heterojunction [94]. The CVD graphene film coated on the patterned Si substrate with an insulating and metallic layer attached perfectly with excellent contact (**Figure 9**). Excellent rectification diode characteristic can be observed for the graphene/n-Si device. The low leakage current can be attributed to uniform contact of the graphene film on Si surface. Photovoltaic action has been observed with illumination of white light. The exciton dissociation can be achieved to obtain a photovoltaic action by creating a suitable barrier height in the graphene/Si heterojunction [92–94]. Recent studies show more than 10% conversion efficiency of CVD graphene/n-Si Schottky junction solar cells [95]. The interesting fact is that by chemical or substitutional doping of graphene allows to tune the electronic state to make p-type or n-type as well as changing the work function. There are enormous potential in this device technology for various optoelectronics application. Such a simple device structure with easy fabrication process can be ideal to integrate for wafer scale production within the existing Si solar cell manufacturing process.

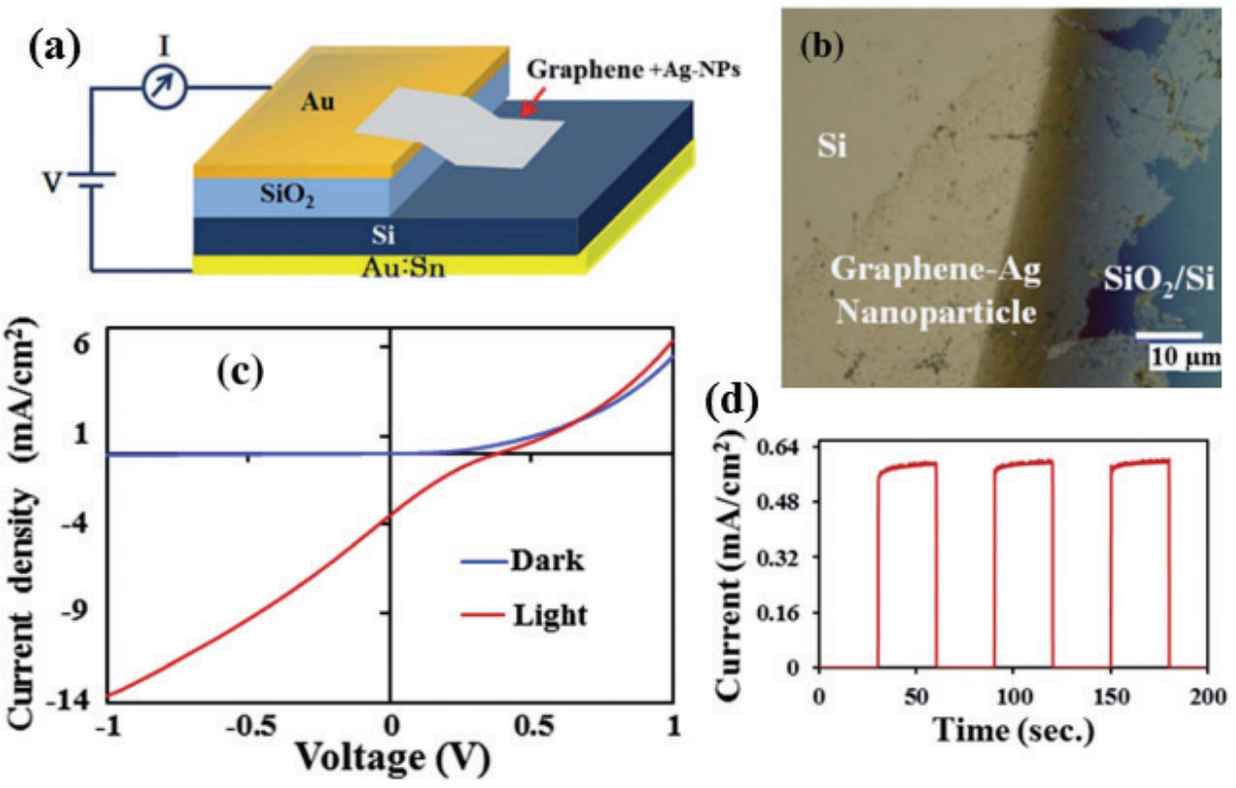

Figure 9. (a) Schematic of fabricated graphene-Si heterojunction. (b) Optical microscope image of silver nanoparticles (AgNPs) coated graphene/Si heterostructure. (c) Current-voltage curves for AgNPs-graphene/n-Si solar cell. (d) Photoresponsivity at 550 nm wavelength. [Reprinted with permission from Ref. [94]].

7.2. Graphene-GaN heterostructure

Integration of CVD graphene with wide bandgap semiconductors has also attracted significant attention for optoelectronic device applications. GaN is one of the most promising wide bandgap semiconductors for applications in optoelectronic and other electronic devices such as light-emitting diodes, laser diodes, solar cells, and high-electron-mobility transistors [95–99]. The transparency of metal oxide conductors is poor in the UV and near UV region, which affects the photodetectors efficiency and brightness of LEDs. In this prospect, a high transparent conductor in the UV region can be the only solution and CVD graphene is the ideal candidate. Another important aspect is low thermal conductivity of metal oxide transparent conductors, reduces the diffusion efficiency of the heat generated during the operation of LEDs. Graphene/GaN heterojunction can be most chemically robust and nondegradable under harsh conditions. The conventional metals like Ni, Pt, and Pd have been used for the fabrication of Schottky junction with GaN. However, diffusion of the metal into semiconductor at elevated temperatures enhances the tunneling of the carriers across the barrier, causing a decrease in thermionic emission current, i.e., lowering of the barrier and hence restricts the high temperature operation of the device. Graphene has been combined with n and p type GaN in lateral and vertical heterostructure to fabricate light emitting diode and photodetectors (**Figure 10**) [98]. The fabrication of light emitting diode has been demonstrated using a tunnel junction configuration such as graphene/n-$In_xGa_{1-x}N$/p-GaN. Similarly, a graphene/GaN-based Schottky UV photodetector has been investigated for higher and faster response than the conventional detectors. UV photodetector device has been fabricated with monolayer CVD graphene. High photoresponsivity has been achieved in the wavelength below 360 nm, corresponding to the band edge absorption of GaN [99]. The current ratio with and without luminescence has been achieved as high as 1.6×10^4. Similarly, multi-layer CVD graphene has been also investigated for photodetector or light-emitting diodes. A method of directly growing graphene films on GaN by the CVD process can be also favorable for fabrication process compatibility. Nevertheless, there are many challenges in graphene-GaN heterojunction fabrications and interface engineering. The important aspect is to understand the graphene/GaN interface physics and transport mechanism for carriers transporting across it. There is plenty of scope to develop 2D (graphene)-3D (Si, GaN, GaAs and other bulk semiconductors) heterostructure for fabrication of energy-efficient devices.

7.3. Graphene-hexagonal boron nitride heterostructure

Significant research interest has been given to develop atomically thin 2D heterostructure of graphene and hexagonal boron nitride (hBN) [100]. hBN can be considered as a structural analogue of graphene, which is composed of alternating boron and nitrogen atoms in a honeycomb lattice rather than the carbon atoms. Graphene with a zero bandgap is a semimetallic as discussed in Section 1, while hBN with a bandgap of ~6 eV is insulating [100–107]. Significant carrier mobility of graphene has been achieved on atomically flat hBN as a dielectric layer for the FET device. hBN with no dangling bond and charge traps make an ideal dielectric material for graphene electronics [104]. It has been also observed that a measurable bandgap can be induced in graphene using hBN as a substrate, opening a new prospect

for the FET fabrication. Recent studies have also revealed that an obvious bandgap can be introduced by in-plane hBN and graphene heterostructures fabrication with a relatively high carrier mobility [106]. In these prospects of vertical heterostructures, the hBN and graphene layer can be transferred individually to fabricate a stack of layers, while a growth process is unavoidable for in-plane heterostructure fabrication. Various CVD approaches have been developed for the fabrication in-plane hBNC hybrid or hBN-graphene heterostructures on the catalyst substrate (e.g., Cu) [106, 107]. These approaches are one-batch growth and two-step patching growth models. Ajayan et al. have demonstrated the synthesis of hBNC film and observed significant influence on electronic property, such as the electrical conductivity and opening a bandgap attributing to the quantum confinement effect or spin polarization at specific C-BN boundaries (**Figure 11**) [106]. Subsequently, hydrogen-induced etching process of graphene or hBN layer has been developed for lateral epitaxial growth of h-BN/graphene structure with sharp interfaces [107]. Temperature-triggered chemical switching growth of in-plane and vertically stacked heterostructures has been also achieved in the same growth process [108]. There are significant potential to control the etched structure and domain formation in an hBN-graphene heterostructure to realize a considerable bandgap. The control in size, shape, interface, and domain structure will be critical for further development of both in-plane and vertical hBN/graphene heterostructure.

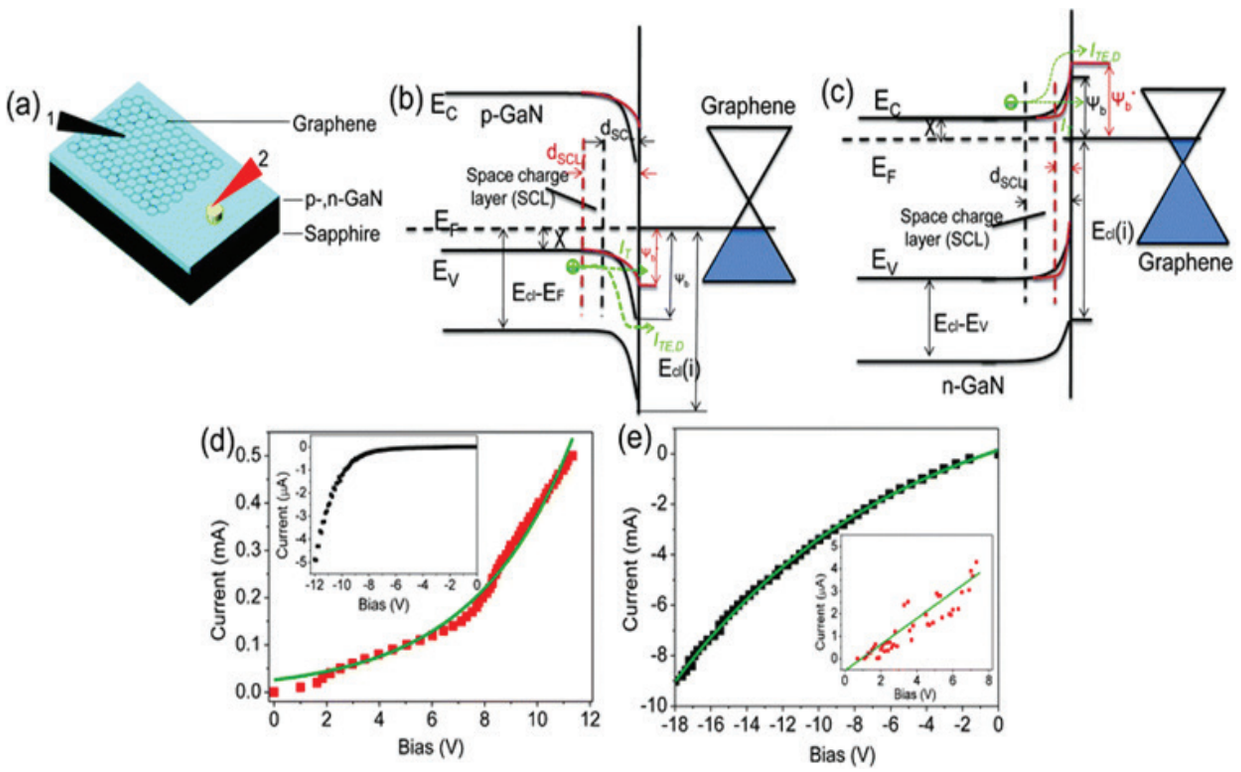

Figure 10. (a) Schematic diagram of graphene-GaN device. (b) and (c): Energy band diagram of graphene/p-GaN and graphene/n-GaN junctions. (d) and (e): Forward current-voltage (*I-V*) characteristics for p-, n-GaN/graphene junctions, respectively; insets of (d) and (e) present the corresponding reverse *I-V* curves. [Reprinted with permission from Ref. [98]].

http://dx.doi.org/10.5772/67514

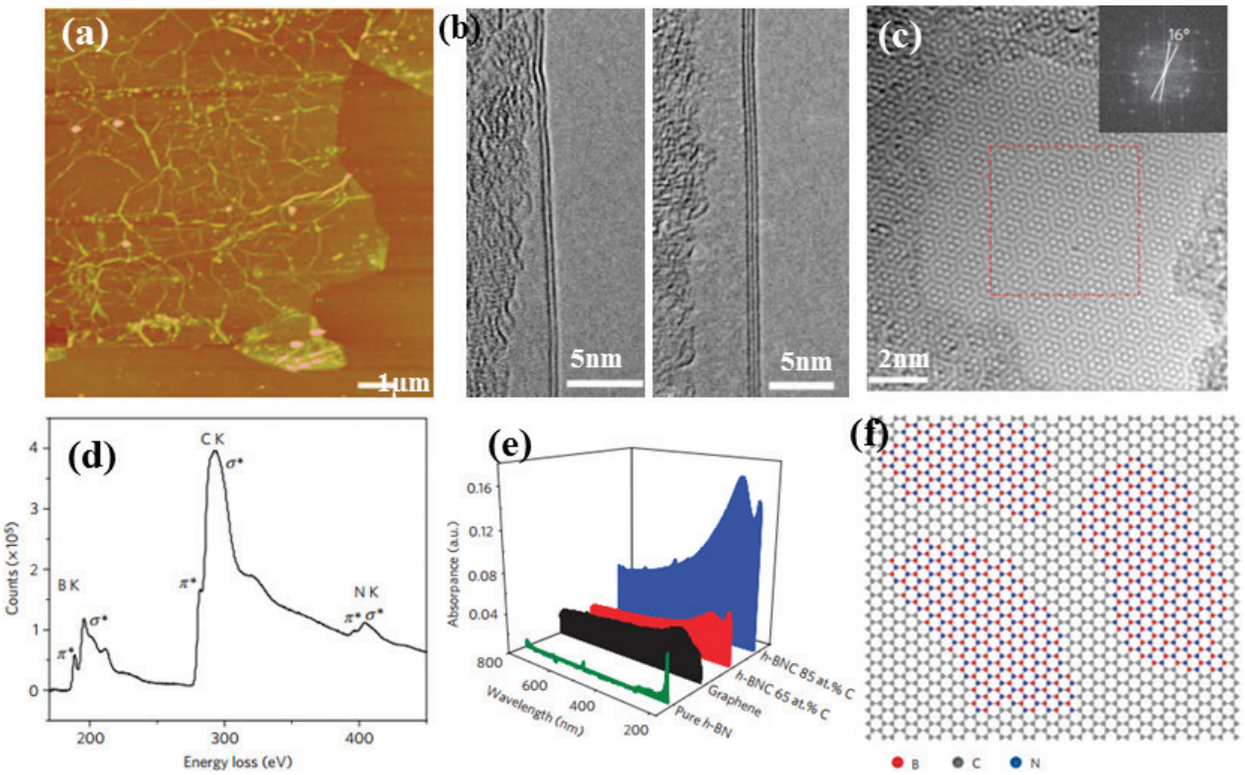

Figure 11. Synthesis of hBNC film by a CVD approach to introduce a bandgap in the hybrid structure. (a) AFM image of the uniform hBNC transferred onto SiO_2/Si substrates. (b) High resolution TEM images presenting the section view of the hBNC film. (c) Moiré patterns of a two layer packing in the hBNC film. (d) EELS spectrum of the hBNC films showing three K-shell excitation edges of B, C and N respectively. (e) UV-Vis absorption spectra of pure hBN, graphene, and hBNC hybrid. (f) Atomic models for the hBNC film. [Reprinted with permission from Ref. [106]].

7.4. Graphene-transition metal dichalcogenides heterostructure

The monolayer transition metal dichalcogenides (TMDC) materials have received significant attention due to the presence of a direct bandgap. TMDCs, such as molybdenum disulfide (MoS_2), tungsten disulfide (WS_2), rhenium disulfide (ReS_2), tungsten diselenide (WSe_2), etc., are the family of compound materials with the generalized formula MX_2, where M is transition metal and X is a chalcogen such as S, Se, or Te. The individual layer of TMDCs consists of three atomic layers in which the transition metal is sandwiched between two chalcogens. The electronic and optoelectronic components fabricated using TMDC-layered materials, such as FET, sensors, and photodetectors, have the potential to substitute conventional Si-based electronics and organic semiconductors [109–111]. TMDC-layered materials have been derived by mechanical exfoliation, liquid exfoliation, solvothermal process, and sulfurization of transition metal-based precursors [112–115]. Among various approaches, the CVD technique is one of the most suitable approaches to obtain wafer-scale uniformity for device fabrication [113, 115]. TMDC materials synthesis by the CVD process is independent of catalyst in contrast to the graphene and hBN CVD synthesis. TMDC layers have been combined with graphene and hBN for the fabrication of transistors, photodetectors, solar cell, sensors,

etc. by exploiting their discrete physical properties [116, 117, 119]. Graphene and TMDCs, such as MoS_2, WS_2, etc., have been combined to fabricate a heterojunction photodetectors. Various other novel devices have been proposed or developed based on heterostructures formed between MoS_2 and graphene. Electronic logic and memory devices have already been constructed from graphene-MoS_2 hybrids [114]. The graphene-MoS_2 heterostructures have also been adopted to demonstrate an extremely high photo-gain and the ultrasensitive sensors fabrication [118, 119]. Considering the significant potential, efforts have been made to grow graphene-TMDCs hybrid structures by a CVD technique (**Figure 12**). Direct synthesis of TMDC layer on graphene has been developed; such large-area van der Waals heterostructures show a significant improvement in photoresponse. In-plane or vertically oriented growth of TMDCs on graphene also has great potential in the hydrogen evolution reaction and sensing device applications.

The beauty of these material systems is that we can design and develop accordingly to achieve something unexpected. Various other layered materials and their heterostructures are emerging with intriguing properties for possible practical nanoelectronics, optoelectronics and energy conversion and storage devices. We expect that the further development of the CVD method will be the forefront of research area to develop graphene and other 2D materials.

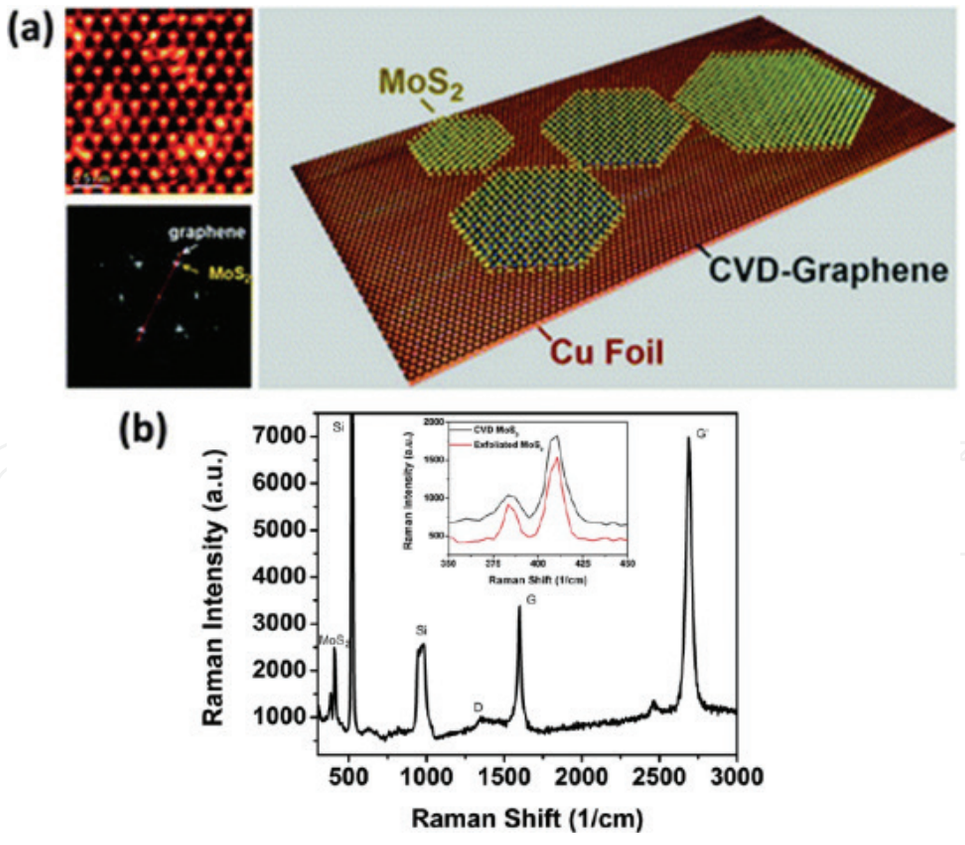

Figure 12. CVD synthesis of monolayer MoS_2 on graphene. (a) TEM images and electron diffraction pattern suggests the Van-der-Waals epitaxy of MoS_2/graphene layers. (b) Raman spectra of the MoS_2/graphene heterostructure. [Reprinted with permission from Ref. [119]].

8. Summary

In the very outset of the chapter, we have discussed the background of graphene research development leading to a new area of research in physics, chemistry, and engineering of 2D crystals. The crystal structure and basic optical, mechanical, electrical, and thermal properties of graphene were presented. Deriving or synthesis of graphene by various approaches was introduced. Among the synthesis processes, a CVD approach has been extensively explored for controlled growth of high quality and large-area graphene for electronic device applications. The thermodynamic and kinetic parameters have a critical role in graphene nucleation and growth process in the CVD method. The pressure and temperature are both key factors for graphene growth, where the kinetic factors, such as gas flow, precursor flow rate, and gas composition pressure also play important roles on graphene quality and structural morphology. We introduced the atmospheric and low pressure CVD technique and growth dynamics of graphene continues film and large single crystals. Catalyst also plays a significant role on the quality of graphene synthesized by the CVD process. We have discussed about the polycrystalline and single crystalline transition metal catalysts and their effect on graphene growth. The surface modification, such as oxidation, plays an important role to reduce nucleation density and thereby achieving centimeter scale single crystal graphene growth in a CVD approach. We also introduced the monolayer graphene growth behavior on a liquid metal catalyst. Next, we discussed about the emerging application of the CVD graphene and fabrication of various heterostructure and hybrid materials. CVD graphene has been integrated with bulk semiconductor such as Si and GaN for fabrication of advanced device structure for solar cell, photodetector, and light-emitting diode applications. In-plane and vertical heterostructures of hBN-graphene have been developed by the CVD process. The control in size, shape, and interface of domain structure will be critical for further development of both in-plane and vertical hBN/graphene heterostructures. Further, graphene and TMDCs (MoS_2, WS_2 etc.) based van der Waals heterostructures have been developed by the CVD process for nanoelectronic, optoelectronic, energy storage, and conversion applications. We expect further development of the CVD method, which will be one of the forefronts of research area to develop graphene and other 2D materials in the coming years.

Author details

Golap Kalita* and Masaki Tanemura

*Address all correspondence to: kalita.golap@nitech.ac.jp

Department of Applied Physics and Engineering, Nagoya Institute of Technology, Japan

References

[1] Novoselov KS, Geim AK, Morozov SV et al., Electric field effect in atomically thin carbon films. Science 2004; **306**: 666–669. DOI: 10.1126/science.1102896.

[2] Peierls RE, Quelques propriétés typiques des corpses solides. Ann. Inst. H. Poincaré 1935; **5**: 177–222.

[3] Landau LD, Lifshitz EM, Statistical Physics, Part I. Pergamon Press: Oxford; 1980. Sections 137 and 138.

[4] Mermin ND, Crystalline order in two dimensions, Phys. Rev. 1968; **176**: 250–254.

[5] Novoselov KS, Geim AK, Morozov SV et al., Two-dimensional gas of massless Dirac fermions in graphene, Nature 2005; **438**: 197–200. DOI:10.1038/nature04233.

[6] Zhang Y, Tan YW, Stormer HL et al., Experimental observation of the quantum Hall effect and Berry's phase in graphene. Nature 2005; **438**: 201–204. DOI:10.1038/nature04235.

[7] Nair RR, Blake P, Grigorenko AN et al., Fine structure constant defines visual transparency of graphene. Science 2008; **320**: 1308. DOI: 10.1126/science.1156965.

[8] Lee C, Wei X, Kysar J W et al. Measurement of the elastic properties and intrinsic strength. Science 2008; **321**: 385–388. DOI: 10.1126/science.1157996.

[9] Geim AK, Novoselov KS, The rise of graphene. Nature Mater. 2007; **6**: 183–191. DOI:10.1038/nmat1849.

[10] Berger C, Song Z, Li X, et al., Electronic confinement and coherence in patterned epitaxial graphene. Science 2006; **312**: 1191–1196. DOI: 10.1126/science.1125925.

[11] Kroto HW, Heath JR, Obrien SC et al. C_{60}: Buckminsterfullerene, Nature 1985; **318**: 162–163.

[12] Original paper in Japanese, translated in: Ozawa E, Kroto HW, Fowler PW, Wassermann E, Phil. Trans. R. Soc. (London) A. 1993; **1**: 343.

[13] Iijima S, Helical microtubules of graphitic carbon. Nature 1991; **354**: 56–58.

[14] Kosynkin DV, Higginbotham AL, Sinitskii A et al., Longitudinal unzipping of carbon nanotubes to form graphene nanoribbons. Nature 2009; **458**: 872–876.

[15] Xu X, Ray R, Gu Y. et al., Electrophoretic analysis and purification of fluorescent single-walled carbon nanotube fragments. J. Am. Chem. Soc. 2004; **126**(40): 12736–12737.

[16] Castro Neto AH, Guinea F, Peres NMR, Novoselov KS, Geim AK, The electronic properties of graphene. Rev. Mod. Phys 2009; **81**: 109–162. DOI: 10.1103/RevModPhys.81.109.

[17] Wallace PR, The band theory of graphite. Phys. Rev. 1947; **71**: 622.

[18] Morozov SV, Novoselov KS, Katsnelson MI et al. Giant intrinsic carrier mobilities in graphene and its bilayer. Phys. Rev. Lett. 2008; **100**. p. 016602.

[19] Balandin AA, Ghosh S, Bao W et al., Superior thermal conductivity of single-layer graphene. Nano Lett. 2008; **8**: 902–907.

[20] Loh KP, Bao Q, Eda G. et al. Graphene oxide as a chemically tunable platform for optical applications. Nature Chem. 2010; **2**: 1015–1024. DOI: 10.1103/PhysRevLett.100.016602.

[21] Novoselov KS, Jiang D, Schedin F et al., Two-dimensional atomic crystals. Proc. Natl. Acad. Sci. 2005; **102**: 10451–10453.

[22] Berger C, Song Z, Li T et al., Ultrathin epitaxial graphite: 2D electron gas properties and a route toward graphene-based nanoelectronics. J. Phys. Chem. B. 2004; **108**: 19912–19916.

[23] Lin YM, Dimitrakopoulos C, Jenkins KA, Farmer DB, Chiu HY, Grill A, Avouris P, 100-GHz transistors from wafer-scale epitaxial graphene. Science. 2010; **327**: 662. DOI: 10.1126/science.1184289.

[24] Stankovich S, Dikin DA, Dommett GHB et al., Graphene-based composite materials. Nature. 2006; **442**: 282–286.

[25] Hummers WS, Offeman RE, Preparation of graphitic oxide. J. Am. Chem. Soc. 1958; **80**: 1339–1339.

[26] Eda G, Fanchini G, Chhowalla M, Large-area ultrathin films of reduced graphene oxide as a transparent and flexible electronic material. Nature Nanotechnol. 2008; **3**: 270–274.

[27] Kalita G, Sharma S, Wakita K et al., A photoinduced charge transfer composite of graphene oxide and ferrocene. Phys. Chem. Chem. Phys. 2013; **15**: 1271–1274.

[28] Kalita G, Wakita K, Umeno M et al., Fabrication and characteristics of solution-processed graphene oxide–silicon heterojunction. Phys. Stat. Sol. RRL 2013; **7**: 340–343.

[29] Avouris P, Dimitrakopoulos C, Graphene: synthesis and application. Mater. Today 2012; **15**: 86–97.

[30] Eizenberg M, Blakely JM, Carbon monolayer phase condensation on Ni(111). Surf. Sci. 1979; **82**: 228–236.

[31] Somani P R, Somani S P, Umeno M, Planer nano-graphenes from camphor by CVD. Chem. Phys. Lett. 2006; **430**: 56–59.

[32] Yu Q, Lian J, Siriponglert S et al., Graphene segregated on Ni surfaces and transferred to insulators. Appl. Phys. Lett. 2008; **93**: 113103.

[33] Kalita G, Masahiro M, Uchida H et al., Few layers of graphene as transparent electrode from botanical derivative camphor. Mater. Lett. 2010; **64**: 2180–2183.

[34] Reina A, Jia X, John H et al., Large area, few-layer graphene films on arbitrary substrates by chemical vapor deposition. Nano Lett. 2009; **9**: 30–35.

[35] Kim K S, Zhao Y, Jang H et al., Large-scale pattern growth of graphene films for stretchable transparent electrodes. Nature 2009; **457**: 706–710.

[36] Li X S, Cai W W, An J H et al., Large-area synthesis of high-quality and uniform graphene films on copper foils. Science 2009; **324**: 1312–1314.

[37] McCarty K F, Feibelman P J, Loginov E, Bartelt N C, Kinetics and thermodynamics of carbon segregation and graphene growth on Ru(001). Carbon 2009; **47**(7): 1806–1813.

[38] Zhang W, Wu P, Li Z, Yang J, First-principles thermodynamics of graphene growth on Cu surfaces. J. Phys. Chem. C 2011; **115**: 17782–17787.

[39] Qi M, Ren Z, Jiao Y, Zhou Y, Xu X, Li W, Li J, Zheng X, Bai J, Hydrogen kinetics on scalable graphene growth by atmospheric pressure chemical vapor deposition with acetylene. J. Phys. Chem. C 2013; **117**(27): 14348–14353.

[40] Kalita G, Matsushima M, Uchida H et al., Graphene constructed carbon thin films as transparent electrodes for solar cell applications. J. Mater. Chem. 2010; **20**: 9713–9717.

[41] Vlassiouk I, Fulvio P, Meyer H et al., Large scale atmospheric pressure chemical vapor deposition of graphene. Carbon 2013; **54**: 58–67.

[42] Lin HC, Chen YZ, Wang YC, Chueh YL, The essential role of Cu vapor for the self-limit graphene via the Cu catalytic CVD method. J. Phys. Chem. C 2015; **119**(12): 6835–6842.

[43] Rosmi MS, Shinde SM, Rahman NDA et al., Synthesis of uniform monolayer graphene on re-solidified copper from waste chicken fat by low pressure chemical vapor deposition. Materials Research Bulletin 2016; **83**: 573–580.

[44] Robert MJ, Michael SA, Graphene growth dynamics on epitaxial copper thin films. Chem. Mater. 2013; **25**: 871–877.

[45] Ivan V, Sergei S, Murari R et al., Graphene nucleation density on copper: Fundamental role of background pressure. J. Phys. Chem. C 2013; **117**: 18919–18926.

[46] Stoffel A, Kovács A, Kronast W, Müller B, LPCVD against PECVD for micromechanical applications. J. Micromech. Microeng. 1996; **6**(1): 20–33.

[47] Kim H, Mattevi C, Calvo MR et al., Activation energy paths for graphene nucleation and growth on Cu. ACS Nano 2012; **6**: 3614–3623.

[48] Hersh H N, The vapor pressure of copper. J. Am. Chem. Soc. 1953, **75**: 1529–1531.

[49] Ayhan ME, Kalita G, Sharma S, Tanemura M, Chemical vapor deposition of graphene on silver foil as a tarnish-resistant coating. Phys. Status Solidi RRL 2013; **7**(12): 1076–1079.

[50] Sun J, Nam Y, Lindvall N et al., Growth mechanism of graphene on platinum: surface catalysis and carbon segregation. Appl. Phys. Lett. 2014; **104**: 4871978.

[51] Jin L, Fu Q, Zhang H, Mu R, Zhang Y, Tan D, Bao X, Tailoring the growth of graphene on Ru(0001) via engineering of the substrate surface. J. Phys. Chem. C 2012; **116**(4): 2988–2993.

[52] Hamilton J C, J. M. Blakely, Carbon segregation to single crystal surfaces of Pt, Pd and Co. Surf. Sci. 1980; **91**: 199–217.

[53] López G, Mittemeijer E, The solubility of C in solid Cu. Scripta Materialia 2004; **51**: 1–5.

[54] Acheson EG, United States Patent; 1896. No. 568323.

[55] Lahiri J, Miller T S, Ross A J, Adamska L, Oleynik I I, Batzill M, Graphene growth and stability at nickel surfaces. New J. Phys. 2011; **13**: 025001.

[56] Sharma S, Kalita G, Hirano R et al., Influence of gas composition on the formation of graphene domain synthesized from camphor. Materials Letters 2013; **93**: 258–262.

[57] Kalita G, Wakita K, Umeno M, Structural analysis and direct imaging of rotational stacking faults in few-layer graphene synthesized from solid botanical precursor. Jap. Jour. Appl. Phys. 2011; **50**: 070106.

[58] Kalita G, Wakita K, Takahashi M et al., Iodine doping in solid precursor-based CVD growth graphene film. J. Mater. Chem. 2011; **21**: 15209–15213.

[59] Zhang Y, Gomez L, Ishikawa F N et al., Comparison of graphene growth on single-crystalline and polycrystalline Ni by chemical vapor deposition. J. Phys. Chem. Lett. 2010; **1**: 3101–3107.

[60] Nie S, Wofford JM, Bartelt NC, Dubon OD, McCarty KF, Origin of the mosaicity in graphene grown on Cu(111). Physical Review B; 2011; **84**: 155425.

[61] Bhaviripudi S, Jia X, Dresselhaus MS, Kong J, Role of kinetic factors in chemical vapor deposition synthesis of uniform large area graphene using copper catalyst. Nano Letters 2010; **10**: 4128–4133.

[62] Hwang C, Yoo K, Kim SJ et al., Initial stage of graphene growth on a Cu substrate. J. Phys. Chem. C 2011; **115**: 22369–22374.

[63] Wood JD, Schmucker SW, Lyons AS et al., Effects of polycrystalline cu substrate on graphene growth by chemical vapor deposition. Nano Lett. 2011; **11**: 4547–4554.

[64] Bae S, Kim HK, Lee, Roll-to-roll production of 30-inch graphene films for transparent electrodes. Nat. Nanotechnol 2010; **5**: 574–578.

[65] Sutter PW, Flege JI, Sutter EA, Epitaxial graphene on ruthenium. Nat. Mater. 2008; **7**: 406–411.

[66] Addou R, Dahal A, Sutter P, Batzill M, Monolayer graphene growth on Ni(111) by low temperature chemical vapor deposition. Applied Physics Letters 2012; **100**: 3675481.

[67] Ago H, Ito Y, Mizuta N et al., Epitaxial chemical vapor deposition growth of single-layer graphene over cobalt film crystallized on sapphire. ACS Nano 2010; **4**: 7407–7414.

[68] Wu T, Ding G, Shen H et al., Triggering the continuous growth of graphene toward millimeter-sized grains. Adv. Funct. Mater. 2013; **23**: 198–203.

[69] Yan Z, Lin J, Peng Z et al., Toward the synthesis of wafer-scale single-crystal graphene on copper foils, ACS Nano 2012; **6**: 9110–9117.

[70] Sharma S, Kalita G, Ayhan ME et al., Synthesis of hexagonal graphene on polycrystalline Cu foil from solid camphor by atmospheric pressure chemical vapor deposition. J. Mater. Sci. 2013; **48**: 7036–7041.

[71] Sharma S, Kalita G, Papon R et al., Synthesis of graphene crystals from solid waste plastic by chemical vapor deposition, Carbon 2014; **72**: 66–73.

[72] Sharma KP, Shinde SM, Rosmi MS et al., Effect of copper foil annealing process on large graphene domain growth by solid source-based chemical vapor deposition. J. Mater. Sci. 2016; **51**(15): 7220–7228.

[73] Papon R, Pierlot C, Sharma S et al. Optimization of CVD parameters for graphene synthesis through design of experiments, Phys. Status Solidi B 2016; 1–7 DOI 10.1002/pssb.201600629

[74] Li J, Wang XY, Liu XR et al., Facile growth of centimeter-sized single-crystal graphene on copper foil at atmospheric pressure. J. Mater. Chem.2015; **C 3**: 3530.

[75] Warner JH, Rümmeli MH, Gemming T, Büchner B, Briggs G, Direct imaging of rotational stacking faults in few layer graphene. Nano Lett. 2009; **9**(1): 102–106.

[76] Wu Y, Chou H, Ji H et al., Growth mechanism and controlled synthesis of AB-stacked bilayer graphene on Cu–Ni alloy foils. ACS Nano 2012; **6**(9): 7731–7738.

[77] Tan L, Zeng M, Zhang T, Fu L, Design of catalytic substrates for uniform graphene films: from solid-metal to liquid-metal. Nanoscale. 2015; **7**: 9105.

[78] Oostinga JB, Heersche HB, Liu X, Morpurgo AF, Vandersypen LMK, Gate-induced insulating state in bilayer graphene devices. Nat. Mater. 2008; **7**: 151–157.

[79] Liu X, Fu L, Liu N et al., Segregation growth of graphene on CuNi alloy for precise layer control. J. Phys. Chem. 2011; **C 115**: 11976–11982.

[80] Takesaki Y, Kawahara K, Hibino H, Okada S, Tsuji M, and Ago H, Highly uniform bilayer graphene on epitaxial Cu–Ni(111) alloy. Chem. Mater. 2016; **28**: 4583–4592.

[81] Wang G, Chen D, Lu Z et al., Growth of homogeneous single-layer graphene on Ni-Ge binary substrate. Appl. Phys. Lett. 2014; **104**: 062103.

[82] Liu N, Fu L, Dai B et al., Universal segregation growth approach to wafer-size graphene from non-noble metals. Nano Lett. 2011; **11**: 297.

[83] Lin T, Huang F, Wan D et al., Self-regulating homogenous growth of high-quality graphene on Co–Cu composite substrate for layer control. Nanoscale. 2013; **5**: 5847.

[84] Rümmeli MH, Zeng M, Melkhanova S et al., Insights into the early growth of homogeneous single-layer graphene over Ni–Mo binary substrates. J. Chem. Mater. 2013; **25**: 3880.

[85] Wu T, Zhang X, Yuan Q et al., Fast growth of inch-sized single-crystalline graphene from a controlled single nucleus on Cu-Ni alloys. Nature Mater. 2016; **15**: 43–47.

[86] Papon R, Sharma KP, Mahyavanshi RD et al., CuNi binary alloy catalyst for growth of nitrogen-doped graphene by low pressure chemical vapor deposition. Phys. Stat. Sol. 2016; RRL **10**: 749–752.

[87] Geng D, Wu B, Guo Y et al., Uniform hexagonal graphene flakes and films grown on liquid copper surface. Proc. Natl. Acad. Sci. 2012; **109**: 7992.

[88] Wang J, Zeng MQ, Tan LF et al., High-mobility graphene on liquid p-block elements by ultra-low-loss CVD growth. Sci. Rep. 2013; **3**: 2670.

[89] Fujita JI, Miyazawa Y, Ueki R et al., Fabrication of large-area graphene using liquid gallium and its electrical properties. Jpn. J. Appl. Phys. 2010; **49**: 06GC01.

[90] Zeng M, Tan L, Wang J et al., Liquid metal: an innovative solution to uniform graphene films. Chem. Mater. 2014; **26**(12): 3637–3643.

[91] Bonaccorso F, Sun Z, Hasan T et al., Graphene photonics and optoelectronics. Nature Photonics 2010; **4**: 611–622.

[92] Li X, Zhu H, Wang K et al., Graphene-on-silicon Schottky junction solar cells. Adv. Mater. 2010; **22**: 2743–2748.

[93] Meng JH, Liu X, Zhang XW et al., Interface engineering for highly efficient graphene-on-silicon Schottky junction solar cells by introducing a hexagonal boron nitride interlayer, Nano Energy 2016; **28**: 44–50.

[94] Ayhan ME, Kalita G, Kondo M et al., Photoresponsivity of silver nanoparticles decorated graphene–silicon Schottky junction. RSC Adv. 2014; **4**: 26866–26871.

[95] Bartolomeo AD, Graphene Schottky diodes: an experimental review of the rectifying graphene/semiconductor heterojunction. Phys. Reports. 2016; **606**: 1–58.

[96] Chandramohan S, Ko KB, Yang JH et al., Performance evaluation of GaN light-emitting diodes using transferred graphene as current spreading layer. Jour. Appl. Phys. 2014; **115**: 054503.

[97] Wang L, Liu W, Zhang Y et al., Graphene-based transparent conductive electrodes for GaN-based light emitting diodes: challenges and countermeasures. Nano Energy. 2015; **12**: 419–436.

[98] Wang L, Zhang Y, Li X et al., Improved transport properties of graphene/GaN junctions in GaN-based vertical light emitting diodes by acid doping. RSC Adv. 2013; **3**: 3359–3364.

[99] Xu K, Xu C, Xie Y et al., Graphene GaN-based Schottky ultraviolet detectors. IEEE Trans. Electron Devices. 2015: **62**: 9.

[100] Li Q, Liu M, Zhang Y, Liu Z. Hexagonal boron nitride-graphene heterostructures: synthesis and interfacial properties. Small. 2016; **12**: 32–50.

[101] Britnell L, Gorbachev RV, Jalil R et al., Field-effect tunneling transistor based on vertical graphene heterostructures. Science. 2012; **335**: 947–950.

[102] Sharma S, Kalita G, Vishwakarma R et al., Opening of triangular hole in triangular-shaped chemical vapor deposited hexagonal boron nitride crystal. Sci. Rep. 2015; **5**: 10426.

[103] Sharma S, Sharma K, Rosmi MS et al., Morphology-controlled synthesis of hexagonal boron nitride crystals by chemical vapor deposition. Cryst. Growth Des. 2016; **16**(11): 6440–6445.

[104] Dean CR, Young AF, Meric I et al., Boron nitride substrates for high-quality graphene electronics. Nat. Nanotechnol. 2010; **5**: 722.

[105] Levendorf MP, Kim CJ, Brown L et al., Graphene and boron nitride lateral heterostructures for atomically thin circuitry. Nature 2012; **488**: 627.

[106] Ci L, Song L, Jin C et al., Atomic layers of hybridized boron nitride and graphene domains. Nat. Mater. 2010; **9**: 430–435.

[107] Gao Y, Zhang Y, Chen P et al., Toward single-layer uniform hexagonal boron nitride–graphene patchworks with zigzag linking edges. Nano Lett. 2013; **13**(7): 3439–3443.

[108] Gao T, Song X, Du H et al., Temperature-triggered chemical switching growth of in-plane and vertically stacked graphene-boron nitride heterostructures. Nat. Commun. 2015; **6**: 6835.

[109] Splendiani A, Sun L, Zhang Y et al., Emerging photoluminescence in monolayer MoS_2. Nano Lett. 2010; **10**: 1271.

[110] Mak KF, Lee C, Hone J, Shan J, Heinz TF, Atomically thin MoS_2: a new direct-gap semiconductor. Phys. Rev. Lett. 2010; **105**: 136805.

[111] Mak KF, He K, Shan J et al., Control of valley polarization in monolayer MoS2 by optical helicity. Nat. Nanotechnol. 2012; **7**: 494.

[112] Yu Y, Li C, Liu Y et al., Controlled scalable synthesis of uniform, high-quality monolayer and few-layer MoS_2 films. Sci. Rep. 2013; **3**: 1866.

[113] Park J, Lee W, Choi T et al., Layer-modulated synthesis of uniform tungsten disulfide nanosheet using gas-phase precursors. Nanoscale. 2015; **7**: 1308–1313.

[114] Roy K, Padmanabhan M, Goswami S et al., Graphene-MoS_2 hybrid structures for multifunctional photoresponsive memory devices. Nat. Nanotechnol. 2013; **8**: 826–830.

[115] Lv R, Robinson JA, Schaak RE, Sun D, Sun Y, Mallouk TE, Terrones M, Transition metal dichalcogenides and beyond: synthesis, properties, and applications of single- and few-layer nanosheets. Acc. Chem. Res. 2015; **48**: 56.

[116] Thangaraja A, Shinde SM, Kalita G et al., An effective approach to synthesize monolayer tungsten disulphide crystals using tungsten halide precursor. Appl. Phys. Lett. 2016; **108**(5): 4941393.

[117] Loan PTK, Zhang W, Lin CT et al., Graphene/MoS_2 heterostructures for ultrasensitive detection of DNA hybridisation. Adv. Mater. 2014; **26**: 4838 .

[118] Liu X, Balla I, Bergeron H et al., Rotationally commensurate growth of MoS_2 on epitaxial Graphene. ACS Nano. 2016; **10**(1): 1067–1075.

[119] Shi Y, Zhou W, Lu AY et al., Van der Waals epitaxy of MoS_2 layers using graphene as growth templates. Nano Lett. 2012; **12**(6): 2784–2791.